

Generating Adversarial yet Inconspicuous Patches with a Single Image

Jinqi Luo,¹ Tao Bai,¹ Jun Zhao,¹ Bo Li,²

¹Nanyang Technological University, Singapore

²University of Illinois at Urbana-Champaign, USA

luoj0021@ntu.edu.sg, bait0002@ntu.edu.sg, junzhao@ntu.edu.sg, lbo@illinois.edu

Abstract

Deep neural networks have been shown vulnerable to adversarial patches, where exotic patterns can result in models wrong prediction. Nevertheless, existing approaches to adversarial patch generation hardly consider the contextual consistency between patches and the image background, causing such patches to be easily detected and adversarial attacks to fail. On the other hand, these methods require a large amount of data for training, which is computationally expensive. To overcome these challenges, we propose an approach to generate adversarial yet inconspicuous patches with one single image. In our approach, adversarial patches are produced in a coarse-to-fine way with multiple scales of generators and discriminators. Contextual information is encoded during the Min-Max training to make patches consistent with surroundings. The selection of patch location is based on the perceptual sensitivity of victim models. Through extensive experiments, our approach shows strong attacking ability in both the white-box and black-box setting. Experiments on saliency detection and user evaluation indicate that our adversarial patches can evade human observations, demonstrate the inconspicuousness of our approach. Lastly, we show that our approach preserves the attack ability in the physical world.

Introduction

Recent years have witnessed the increasing trend of Deep Neural Networks (DNN) applied in many domains. However, despite its popularity, DNN has been shown susceptible to Adversarial Examples (AE) where negligible noise perturbations (Szegedy et al. 2014) can successfully fool the classifier. Such small perturbations can lead DNN’s prediction into either an intentionally-chosen class (targeted attack) or classes that are different from the true label (untargeted attack). Extensive researches have studied to generate strong AEs (Moosavi-Dezfooli, Fawzi, and Frossard 2016; Carlini and Wagner 2017; Papernot et al. 2016; Su, Vargas, and Sakurai 2019; Liu et al. 2019b). To make attacks applicable in physical world, adversarial patch-based attack (Kurakin, Goodfellow, and Bengio 2016; Brown et al. 2017; Wiyatno and Xu 2019; Li, Schmidt, and Kolter 2019) are proposed. Different from adversarial perturbations added to whole images, such attacks modify pixels within a re-

stricted region to generate malicious patches and fool the DNN model. The existence of adversarial patches intensifies people’s concerns on the security of deep learning based applications in real world, such as auto-driving system and identity recognition devices.

To launch an effective and strong attack in physical world, adversarial patches break the l_p norm limitations for adversarial perturbations. The consequence is that existing adversarial patches are usually ended being noticeable for the human observer because of their exotic appearance. Note that, if the attacks are easily detected, the attacks will fail in practice with a great chance. So it is significant for adversaries to consider adversarial patches that are inconspicuous or even invisible to human. Nevertheless, this haven’t attracted much attention and few works appear. Liu et al. observed there are often scrawls and patches on traffic signs in the real world, and firstly attempted to enhance the visual fidelity while trying to preserve the attack ability. Jia et al. encoded the malicious information as watermarks to evade detection.

In addition, existing methods (Brown et al. 2017; Liu et al. 2019a) require a large amount of quality data (e.g. ImageNet) for training, which is computationally expensive and time-consuming. Apart from the high demand of computation resources, data scarcity is becoming an increasingly troublesome problem. Sensitive data under privacy protection are often out of reach in many situations for training adversaries. The above two problems make current adversarial patch generation methods inappropriate in practice.

Towards bridging research gaps mentioned above, we propose a GAN-based approach to generate Adversarial yet Inconspicuous Patches (AIP) trained from one single image. Our approach captures the most sensitive area of the victim image, and applies adversarial patches generated with well-crafted objective functions. The goals of AIP are (1) crafting adversarial patches with limited data, and (2) evading human detection while keeping attacks successful. Through experiments in digital settings, adversarial patches generated by AIP achieved high attack success rates. Saliency detection and human evaluation shows that our less-noticeable patches highly reduced the risk of being detected before attacks. In the last, we apply AIP in physical scenarios to inspire future directions on developing real-world patch attack.

In summary, the key contributions of this paper are as follows:

- To the best of our knowledge, we are pioneering to study on generating inconspicuous adversarial patches to evade detection. We propose a novel approach AIP to generate such adversarial patches from one single image while preserving strong attack ability.
- Through extensive experiments, our approach performs well in both white-box and black-box settings, and can be used in physical attack. Meanwhile, we demonstrate that such adversarial patches are able to evade detection, which increases the potential threats of adversarial patches.

Related Work

In this section, we review the prior work of adversarial attacks and adversarial example detection.

Adversarial Attacks

Adversarial examples were first discovered (Szegedy et al. 2014). Szegedy et al. added some imperceptible noises on the clean image, and misled well-trained classification models successfully. This greatly attracted researchers' attention and extensive attacks are developed since then. According to the restrictions when crafting adversarial examples, adversarial examples can be roughly categorized into three types: perturbation-based, patch-based, and unrestricted adversarial examples.

Adversarial Perturbation. Following (Szegedy et al. 2014), more perturbation-based attacks are proposed in recent years. Goodfellow, Shlens, and Szegedy proposed Fast Gradient Sign Method (FGSM) to generate adversarial examples fast and effectively. Tramèr et al.; Kurakin, Goodfellow, and Bengio enhanced FGSM with a randomization step or multiple gradient steps. More representative attacks like (Papernot et al. 2016; Moosavi-Dezfooli, Fawzi, and Frossard 2016; Carlini and Wagner 2017; Madry et al. 2018) explore possibilities of attacks in different ways. But these methods shares common restrictions on the norm of perturbations, where a noise budget ϵ is given. The goal of such attacks is to find adversarial examples with small ϵ so that the perturbations are ensured to be imperceptible to human eyes.

Adversarial Patch. Adversarial patches are inspired by the pixel attack (Su, Vargas, and Sakurai 2019) that changes only one pixel to arbitrary value. However, the success rate of pixel attacks is usually low because the change is minor, especially for high resolution images. Patch-based attacks break the restriction in pixel attack that only one pixel is replaced, which makes the attack more efficient and applicable in physical world. Adversarial patches, were first generated by (Brown et al. 2017) in 2017. By masking relatively small patches on the image, such attack causes classifiers to ignore other scenery semantics and report a false prediction. Eykholt et al. generates robust patches under different physical conditions to fool the classification of real-world road sign. Some authors also investigated adversarial patches for attacking object detection models tested in digital settings

(Liu et al. 2019c) and physical settings (Thys, Ranst, and Goedeme 2019; Lee and Kolter 2019).

Though existing adversarial patches have great attack ability, they are highly conspicuous. If there are any detection, such patches will be spotted, leading to failures of the attacks. To make adversarial patches bypass potential detection, Liu et al. generates more realistic patches with Generative Adversarial Nets (GAN) (Goodfellow et al. 2014). In (Jia et al. 2020), the malicious area is disguised as watermarks to evade detection. Their approaches assume that people's understanding of the image content is not affected by such semi-transparent perturbations and hence people's consciousness will not be aroused.

Unrestricted Adversarial Examples. When generating the above discussed adversarial examples, there are always restrictions like the perturbations' norm or the patch size. The reason that such restrictions exist is that attacks naturally have to be undetectable or difficult to detect. Unrestricted adversarial examples occur along with the quick development of GAN, since identifying images synthesized GAN from natural images in a glance becomes impossible for human. Unrestricted adversarial examples are first discovered by (Song et al. 2018). They employed GAN to approximate the distribution of training data, then searched for adversarial examples within the distribution. (Qiu et al. 2019) directly manipulates latent vectors of images which contains semantic information, and inputs the latent vector to GAN so that adversarial examples are disguised as natural images.

Adversarial Example Detection

In practice, adversarial example detection is one of effective defenses on adversarial examples. Lu, Issaranon, and Forsyth assumed adversarial examples produce different patterns of activation functions, proposed to append a SVM classifier to detect adversarial perturbations. Similarly, Metzen et al.; Meng and Chen attached subnetworks which are trained for classification of benign and malicious data. Statistics of convolutions in CNN-based networks are used for detection in (Li and Li 2017). Feature squeezing is also an effective approach to detect adversarial perturbations (Xu, Evans, and Qi 2017).

However, to our best knowledge, the current research still lacks comprehensive studies on automatic detection of adversarial patches trained on large-scale datasets. One possible reason is that existing adversarial patches preferably emphasize on the attack ability, so they cannot even escape from human observation. Our paper would be a pioneering work in which adversarial patches are imperceptible to some extent while preserving strong attack ability. We hope our work could shed some light on benchmarks of inconspicuous patch-based attacks in the future, and inspire researchers to develop defense algorithms robust to adversarial patches.

Our Approach

In this section, we first introduce the problem definition, then elaborate the framework and formulation of our proposed patch-based attack named AIP.

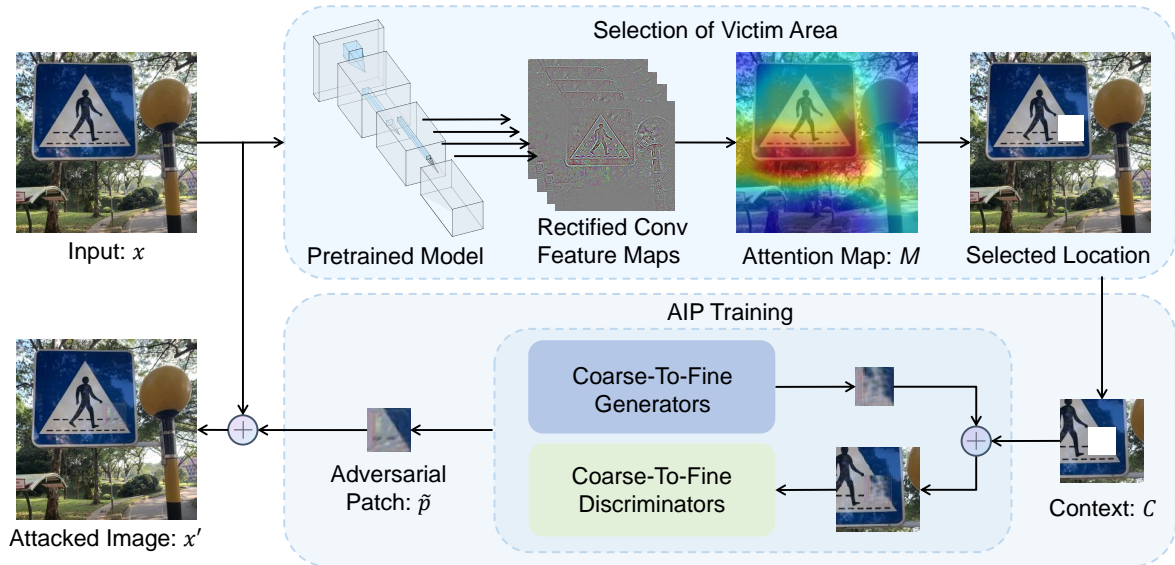


Figure 1: The Overall Structure of Our Approach

Problem Definition

Patch-based attack is created by completely replacing a part of original image. Given a victim image x of size (H, W) , we aim to generate an adversarial patch p of size (h, w) , which can result in prediction errors of well-trained target models f . We attach p with a location mask $m \in \{0, 1\}_{(H \times W)}$ onto the victim image. The new image is given by

$$x' = m \otimes p + (1 - m) \otimes x, \quad (1)$$

where \otimes is the element-wise multiplication for matrices, and p is padding to same size of x . For the ease of reading, we replace the masking process described in Equation 1 with an abstracted notion \oplus in the following sections:

$$x' = p \oplus x. \quad (2)$$

With such adversarial patch, the prediction of x' is expressed as $f(x')$, which differs from the original prediction $f(x)$.

AIP Framework

The overview of our framework is illustrated in Figure 1. Given a target image, we first generate an attention map with target models in white-box setting and pretrained models in black-box setting, which captures the sensitivity of models' output with respect to the input image. The areas in red are better candidates recommended to attack than areas in blue. After deciding the victim area, we take a larger patch containing the recommended location, which we call the context C . Then, the victim area and its surrounding context will be sent to the core component to generate adversarial patches. Here we take the attack ability and visual fidelity into account, and adopt a coarse-to-fine process using GAN with different scales for inconspicuous adversarial patch generation. Different from existing methods, our approach takes only one single image as training data. Inspired by (Shaham, Dekel, and Michaeli 2019; Shocher et al. 2019), we adopt a

multi-scale GAN so that the generator could approximate the internal statistics within the single image and produce realistic patches.

Multi-Scale Patch Generation. In our approach, we deploy a series of generator-discriminator pairs $\{(G_0, D_0), \dots, (G_K, D_K)\}$, where K is the total number of scales in the structure. As shown in Figure 2, these generator-discriminator pairs are trained against an image pyramid of p and C . Correspondingly, the image pyramid is expressed as $\{(p_0, C_0) \dots (p_K, C_K)\}$, where p_i and C_i are downsampled version of p and C with a factor r^{K-i} ($0 < r < 1$).

In every scale, we execute adversarial training for generators and discriminators. The generator G_i is expected to produce realistic patches, and the discriminator attempts to distinguish generated samples from p_i . Since our approach requires the generated patches to be consistent with original images, the input of discriminator is the surrounding context C_i with the intermediate patches p_i placed right at the center of context. During training, the background information will be encoded to the generator progressively.

As we can see from Figure 2, the generation of patches happens in a sequential way, which starts at the coarsest scale and ends at the finest scale. Except the first generator, other generators take the output from coarser scale and noises as the new input. Specifically, the generated patch from coarser scales is upsampled and serves as a prior for the generators in finer scales. Random noises z are used for diversity of generation. Finally, our generator at the finest scale G_K will output adversarial patches \tilde{p} of size (h, w) on a prospective location L of the victim image x .

Objective Functions

As presented above, each generator is coupled with a Markovian discriminator (Li and Wand 2016), and there is no dif-

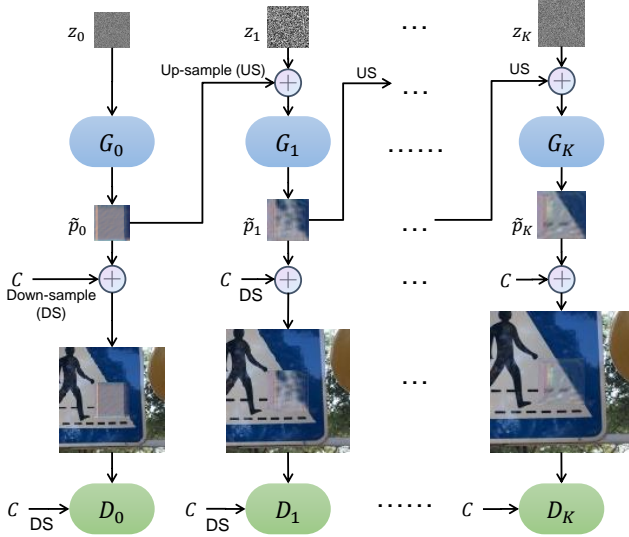


Figure 2: Structure of coarse-to-fine pipeline

ference for training in different scales. So we take the i_{th} scale to elaborate the training details.

We denote the output of G_{i-1} as \tilde{p}_{i-1} , then the input for G_i is

$$\tilde{p}_i = G_i(z_i, (\tilde{p}_{i-1})^\uparrow), \quad (3)$$

where \tilde{p}_{i-1}^\uparrow is the upsampled patch of \tilde{p}_{i-1} .

The adversarial loss (Goodfellow et al. 2014) can be written as

$$\mathcal{L}_{\text{GAN}} = \mathbb{E}_{p_i \sim x} \log \mathcal{D}(p_i, C_i) + \mathbb{E}_{z_i \sim \mathcal{P}_z} \log(1 - \mathcal{D}(G(z_i, \tilde{p}_{i-1}), C_i)), \quad (4)$$

where \mathcal{P}_z is a prior for noises. The discriminator \mathcal{D} for AIP has two functionalities: (1) distinguishing the generated sample $G(z_i, \tilde{p}_{i-1})$ from the original patch p_i , and (2) making sure the patch is consistent with the context C .

The loss for fooling target model f in untargeted attacks is

$$\mathcal{L}_{\text{adv}}^f = \mathbb{E}_x \ell_f(x \oplus \tilde{p}_i^\uparrow, y), \quad (5)$$

where ℓ_f denotes the loss function used in the training of f , and y is the true class of x . Note that it is feasible to replace y with labels of other classes to perform targeted attacks.

To stabilize the training of GAN, we add the reconstruction loss

$$\mathcal{L}_{\text{rec}} = \|G_i(z_i, \tilde{p}_{i-1}) - p_i\|^2. \quad (6)$$

We also add a total variation loss

$$\mathcal{L}_{\text{tv}} = \sum_{a=0}^h \sum_{b=0}^w (|p_i^{(a+1,b)} - p_i^{(a,b)}| + |p_i^{(a,b+1)} - p_i^{(a,b)}|) \quad (7)$$

as a regularization term to ensure that the texture of generated patches is smooth enough. Finally, the full objective function in i_{th} scale can be expressed as

$$\mathcal{L} = \mathcal{L}_{\text{adv}}^f + \alpha \mathcal{L}_{\text{GAN}} + \beta \mathcal{L}_{\text{rec}} + \gamma \mathcal{L}_{\text{tv}}, \quad (8)$$

where α , β and γ are to balance the relative importance of each loss. Then we train our generator and discriminator by solving the min-max game as

$$\operatorname{argmin}_{G_i} \max_{D_i} \mathcal{L}(G_i, D_i). \quad (9)$$

As shown in Algorithm 1, starting from the coarsest scale, our generative models is trained sequentially. For each scale, the GAN is fixed once trained. Then the training repeats in next scale until the finest scale.

Algorithm 1 AIP Generation Process

Input: Single real image x , the victim classifier f
Output: Generator G to generate adversarial patches \tilde{p}

- 1: Obtain the attention heatmap M ;
- 2: Select victim location m ;
- 3: Crop the original patch p and surrounding context C ;
- 4: **for** K scales **do**
- 5: **for** N epochs **do**
- 6: **for** S_D steps **do**
- 7: $W_{D_k} \leftarrow W_{D_k} + \nabla_{D_k} \mathcal{L}$;
- 8: **end for**
- 9: **for** S_G steps **do**
- 10: $W_{G_k} \leftarrow W_{G_k} - \nabla_{G_k} \mathcal{L}$;
- 11: **end for**
- 12: **end for**
- 13: **end for**
- 14: $\tilde{p} = G_K(z_K, G_{K-1}(z_{K-1} \dots (G_1(z_1, G_0(z_0, \vec{0}))) \dots))$;

Experiment Results

In this section, we conducted a series of experiments to evaluate the attack ability in both white-box and black-box settings. To assess how well the generated patches are inconspicuous, we do comparisons of saliency detection and human evaluation on generated adversarial patches. We also attempt physical attacks to evaluate practical effectiveness of our approach.

Implementation Details

We adopt similar architectures for generators (Isola et al. 2017; Zhu et al. 2017). For discriminator, we use a fully convolutional network with 5 conv-blocks (Shaham, Dekel, and Michaeli 2019). In adversarial training, we use WGAN-GP loss in (Gulrajani et al. 2017) as it is found to produce better results with stable training. Since C&W loss (Carlini and Wagner 2017) is proved to be effective to generate strong adversarial examples, we adopt it as our attack loss $\mathcal{L}_{\text{adv}}^f$. Our approach is implemented on a workstation with four GPUs of NVIDIA GeForce RTX 2080 Ti. During the training of AIP, we set 2000 epochs for each scale where the coarsest scale length is 0.75 times of the original patch length. The optimizer for all generators and discriminators is Adam with learning rate 0.0005. All images used in our experiments are normalized to the range of $[-1, 1]$.

Class Index/Name	White-box attack		Black-box attack		
	InceptionV3	GoogLeNet	MNASNet	MobileNet	Robust MobileNet
283 Persian Cat	100.00%	99.22%	85.62%	90.66%	80.33%
340 Zebra	98.53%	99.36%	85.58%	90.38%	74.40%
417 Balloon	99.52%	99.19%	79.68%	90.19%	82.70%
527 Desktop Computer	99.72%	99.20%	82.23%	90.71%	77.86%
532 Table	99.95%	99.19%	86.13%	90.09%	87.09%
604 Hourglass	99.99%	99.20%	82.12%	90.59%	80.39%
717 Pickup Truck	99.97%	99.31%	85.34%	91.06%	75.65%
919 Street Sign	98.30%	99.21%	82.27%	90.10%	84.92%
964 Potpie	99.88%	99.30%	83.81%	90.85%	80.01%
975 Lakeside	99.91%	99.30%	84.00%	89.96%	71.85%
Average	99.58%	99.25%	83.68%	90.46%	79.52%

Table 1: White-box and Black attack success rate for every category’s 10 models. The white-box is conducted on InceptionV3 and black-box is then conducted on GoogLeNet, MNASNet (multiplier of 1.0), MobileNetV2, and MobileNetV2 with L2 robust training ($\epsilon = 3$). The statistics indicates that our approach has strong attacking ability in white-box and black-box settings.

White-box and Black-box Attack

In this section, our data are randomly sampled from ImageNet (Deng et al. 2009). Due to resource limitation, it is impossible for us to use thousands of images in our experiments. So we first choose 10 classes from ImageNet, and sample 10 images in each class (see details in Table 1). In total, 100 images are used as our evaluation set. To assess the attack capability of adversarial patches generated by our approach, we conduct experiments in white-box setting and black-box setting respectively.

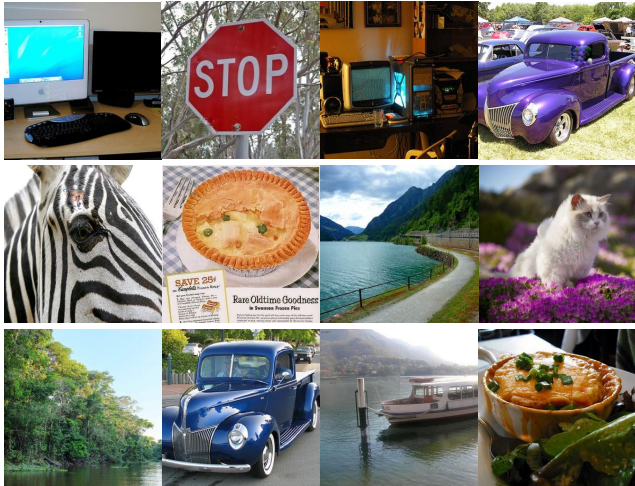


Figure 3: Selected adversarial patches generated by our approach. At the first glance, most of the patches are inconspicuous to human observers.

White-box Attack. We use Inception V3 (Szegedy et al. 2015b) as the target model for white-box attacks. The size of generated patches is fixed as (3,40,40), which cover less than 2% area of the input images (the input size of Inception V3 is (3,299,299)). Since the training of our approach

runs on one single image, we trained 100 models with all images sampled above. Within each trained model, we generated 1,000 adversarial patches for evaluation.

The categorical white-box success rates are shown in the first column of Table 1. We can see that those attacks are of very high success rates with a 99.58% on average. A few randomly selected examples are illustrated in Figure 3.

Transferability for Black-box Attack. In black-box setting, the adversaries are not allowed to access the target models. To perform attacks, they can only produce adversarial patches with known models, then use these patches for attack. Thus we simply use the 100,000 adversarial examples generated in last experiment, in which the target model is Inception V3. There are four different target models for evaluation, namely GoogLeNet (Szegedy et al. 2015a), MNASNet (Tan et al. 2019) with a depth multiplier of 1.0, MobileNetV2 (Sandler et al. 2018), and the L2 adversarially-trained MobileNetV2 ($\epsilon = 3$). Note that the robust accuracy of adversarially trained MobileNetV2 is 50.40% (Salman et al. 2020) while the same model’s accuracy on AIP falls below 20%. This indicates that our generated patches are not traditional adversarial perturbations. The success rates for black-box attack are also shown in Table 1. As expected, there is a drop on success rates. But it is worth noting that the average success rate on GoogLeNet is almost the same as that on Inception V3. The reason might be they both have inception modules. On MNASNet, MobileNetV2 and adversarially trained MobileNetV2, our patches are impressive enough as the success rates of which are 83.68% 90.46% and 79.52% respectively. As discussed above, our approach shows an outstanding attacking ability in the white-box setting and demonstrates a satisfying result when applied on black-box attacks. Note that the reason we don’t compare with other patch methods is because there is no similar work focusing on adversarial patch generation from one single image.

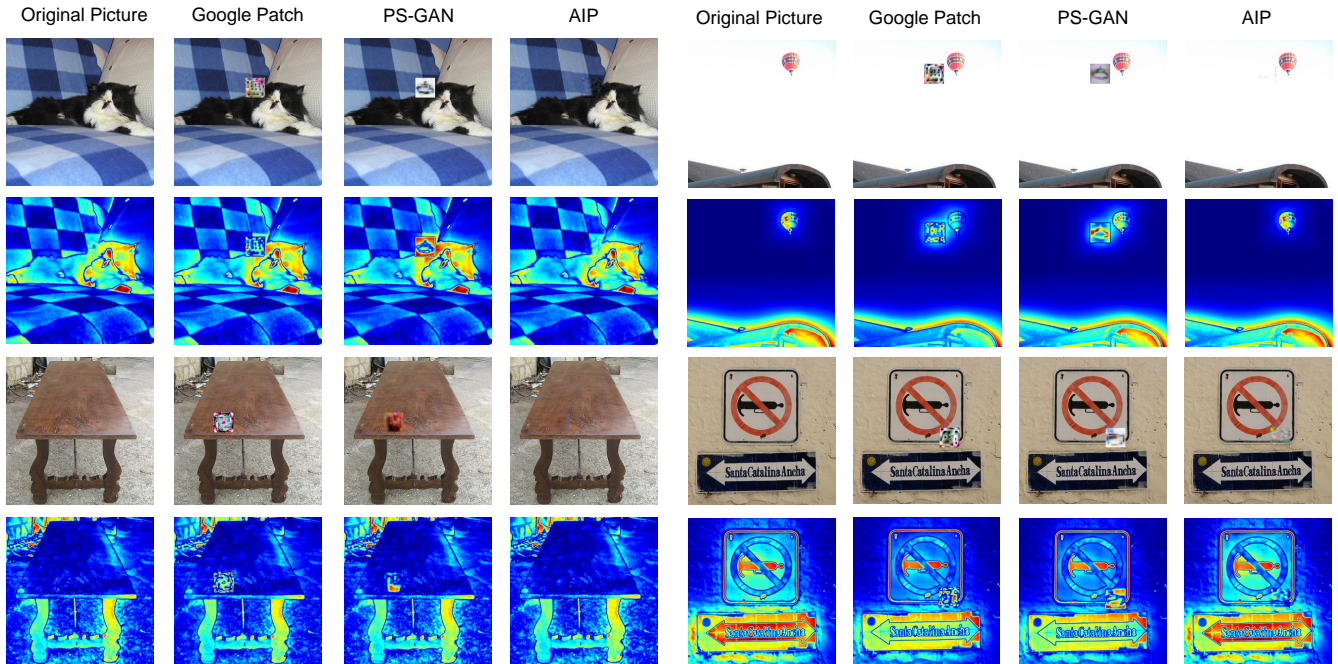


Figure 4: Examples of saliency detection for adversarial patches. We can see that our approach well reserves the visual consistency compared to other approaches and does not trigger the saliency detection significantly.

Detection Risk Evaluation

In this section, we evaluate the risks of adversarial patches prone to detection from two aspects. Qualitatively, we use visual saliency map to show the human-simulated focus area. Quantitatively, we conduct a user study to identify if there exists adversarial patches.

Visual Saliency Detection. Saliency detection (Montabone and Soto 2010) is developed based on a biologically-inspired attention system. The simulated human’s attention is highlighted in the target image to indicate observer’s interest at first glance. With saliency map, we can easily approximate what people are focusing when they take a glance at the image.

We compare our synthetic patches with Google Patch (Brown et al. 2017) and PS-GAN (Liu et al. 2019a) since these patch-based adversaries are targeted at image classifiers for digital images, while including original images as the baseline. Note that in each background image, all the patches are attached in the same location for fairness. Some examples and their saliency maps are illustrated in Figure 4. We can see that patches generated by other two methods are easily spotted, and there are evident square areas at corresponding locations in saliency maps. This means these patches have a high probability to be detected at people’s first glance. In contrast, adversarial patches generated by our approach can be hardly identified from saliency maps. This indicates that patches from our approach are relatively inconspicuous under human observation at first glance.

User Evaluation. In this section, we conducted a user study to evaluate the detection risks of adversarial patches.

Similarly we compare our approach with Google Patch and PS-GAN. Specifically, we prepare 100 images, in which 50 images are with AIP adversarial patches, and the rest images are each attached with a patch from PS-GAN or Google Patch, or are simply natural images. These images are split into five Question Sets and in each of the Set there are 20 images. The participants are asked to pick up one question set and label all images on which they found the existence of synthetic patches. In total we collected 102 answer sheets, in which the users are at least of undergraduate education level. We calculated the rates of images with patches that are labeled and the statistics are summarized in Table 2. As we can see, patches produced by Google Patch and PS-GAN are of significantly higher probability to be detected while ours is much lower. Though our approach cannot beat natural images on identified rates, it is much better than existing methods. To summarize, our approach greatly reduces the detection risks.

Natural Image	Google Patch	PS-GAN	AIP
12.15%	93.63%	89.90%	36.96%

Table 2: Average percentage of synthetic patches on the background images detected in user evaluation.

Further, we investigate if contents of adversarial patches will influence the detection. In our opinion, there are two main factors leading to an inconspicuous patch. Firstly, there should be sufficient consistency between patches and backgrounds. If high contrasts are found by observers, patches

will catch his/her visual attention immediately. Secondly the content of patches should look natural, otherwise the non-sense appearance will induce observers to figure them out. To show this, we conduct a proof-of-concept experiment by asking participants to grade on the patches’ natural-looking appearances. we prepare 120 images, in which 30 of them are the original image, 30 for the original image attached by Google Patch, 30 for PS-GAN patch, and 30 for AIP patch. The best should be graded with 4 and the worst graded with 1 in each group of four approaches. We collected 103 answer sheets, in which the users are at least of undergraduate education level. The average scores are shown in Table 3. As expected, our approach earns a much closer score to natural images. What is more, we notice there exists a negative correlation between Table 2 and Table 3, which supports our claim that AIP is more inconspicuous and less detectable to observers compared to existing approaches.

Natural Image	Google Patch	PS-GAN	AIP
3.548	1.554	1.912	3.078

Table 3: Results of human evaluation grades on natural-looking appearance for each approach.

Physical Attack in Real World

In this section, we conduct an experiment to show the attacking effectiveness of our approach in real-world settings. We choose five real-world traffic sign boards beside the streets: three are Pedestrian-Ahead, one is Speed-Limit-15, and one is No-Entrance. For implementation, we first take one photo from each board by horizontal angles $\theta = \{0^\circ\}$ and $d = \{1m\}$ (camera orthodox and closest to signs). These five traffic sign photos are correctly classified by InceptionV3 as "920 Traffic Sign". Then we trained our models on these 5 images. For enhancing the real-world attack capability of AIP, we add the loss function (Equation 8) with a non-printability score (Sharif et al. 2016)

$$\mathcal{L}_{print} = \sum_{p' \in \tilde{p}} \prod_{a \in A} |p' - a|, \quad (10)$$

where A is the available collection of printable RGB values of $[0, 1]^3$ and p' is a pixel in our adversarial patch \tilde{p} . This is to make sure that the colors of our digital adversarial patches are printable from printers.

When the training is done, we printed out the generated adversarial patches. The model of printer we used is HP Color LaserJet CP3525dn. Then to ensure the fairness of natural lighting conditions, on another day we stuck printed patches on the signs correspondingly and took photos of each sign at almost the same time in a day when it is firstly sampled. Finally we took 195 photos with various horizontal angles $\theta = \{-30^\circ, -15^\circ, 0^\circ, 15^\circ, 30^\circ\}$ and distances $d = \{1m, 2m, 3m, 4m\}$. All photos are taken by iPhone Xs Max.

After sampling we resized photos and normalize them following the regular ImageNet approach, after which photos will be recognized by an ImageNet-trained InceptionV3.

The classification statistics shows that, among 162 photos after attack, there are 60 photos that successfully fool the classifier to make the road sign unrecognized. We show some successful examples of physical attack in Figure 5.

Considering AIP is designed and developed on digital settings, we see that it remains intriguing on how to build stronger yet inconspicuous attack with limited real-world data in physical attack settings. Nevertheless, we can safely conclude that at least our approach has the potential to attack the image classifiers after printing out and sticking to some real-world objects like road signs.

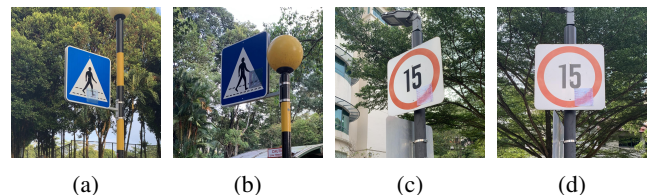


Figure 5: Examples of our physical attack. Traffic Signs are classified as (a) 575 Golf Cart, (b) 733 Pole, (c) 999 Toilet Tissue, and (d) 580 Green House.

Patch or Perturbation?

Images with inconspicuous patches are naturally similar to the original images. Adversarial perturbations are strictly within a small L_p norm ball, which also makes them imperceptible to observers. But note that our approach is not generating adversarial perturbations. To show the differences, we randomly choose 15 target images and their corresponding AIPs generated by our approach. We also perform PGD attack ($\epsilon = 8$) (Madry et al. 2018) and obtain the adversarial images. Then we calculate the AIPs’ pixel difference with original patches, and PGD-attacked samples’ pixel difference with original images. The distributions of pixel differ-

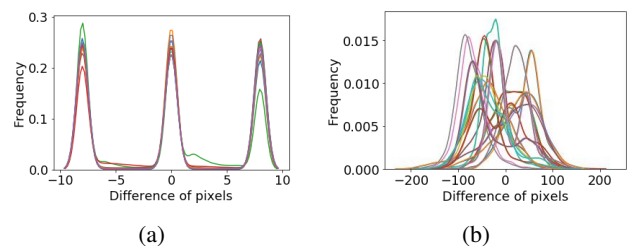


Figure 6: Examples of value distribution obtained by (a) subtracting PGD noise ($\epsilon = 8$) with original sample, and (b) subtracting AIP patch with original patch.

ence are shown in Figure 6. We can see that there are observable distributional differences between PGD attack whose value gaps are restricted within a given radius and our approach where there exists no such perturbation constraint.

Conclusion

In this paper, we propose an approach of GAN-based adversarial networks trained with only one image to produce

adversarial patches. Different from existing works, we consider the consistency between patches and original images to evade detection from observers. Our approach employs multiple scales of generators with discriminators to generate patches in a coarse-to-fine way. To equip our approach with stronger attacking capability, we consider the perceptual sensitivity of victim model by developing model attention mechanism. Through extensive experiments, our approach shows satisfying attack capabilities, black-box transferabilities, and deployable potential in real-world settings. What's more, our approach is proved to be effective on reducing detection risks by qualitative and quantitative evaluations. We address the potential threats of inconspicuous adversarial patches in real world practices. However, we still need to consider how to further deal with the adversarial patch's trade-off between maliciousness and inconspicuousness. In the future work, we will focus on maximizing the real-world attack capability of adversarial patches while reserving least risks of being detected.

References

- Brown, T. B.; Mané, D.; Roy, A.; Abadi, M.; and Gilmer, J. 2017. Adversarial Patch. *ArXiv abs/1712.09665*.
- Carlini, N.; and Wagner, D. 2017. Towards Evaluating the Robustness of Neural Networks. *2017 IEEE Symposium on Security and Privacy (SP)* doi:10.1109/sp.2017.49. URL <http://dx.doi.org/10.1109/SP.2017.49>.
- Deng, J.; Dong, W.; Socher, R.; Li, L.-J.; Li, K.; and Fei-Fei, L. 2009. ImageNet: A Large-Scale Hierarchical Image Database. In *CVPR09*.
- Eykholt, K.; Evtimov, I.; Fernandes, E.; Li, B.; Rahmati, A.; Xiao, C.; Prakash, A.; Kohno, T.; and Song, D. 2018. Robust Physical-World Attacks on Deep Learning Visual Classification. In *Proceedings of the IEEE Conference on Computer Vision and Pattern Recognition (CVPR)*, 1625–1634. doi:10.1109/CVPR.2018.00175.
- Goodfellow, I.; Shlens, J.; and Szegedy, C. 2015. Explaining and Harnessing Adversarial Examples. In *International Conference on Learning Representations*. URL <http://arxiv.org/abs/1412.6572>.
- Goodfellow, I. J.; Pouget-Abadie, J.; Mirza, M.; Xu, B.; Warde-Farley, D.; Ozair, S.; Courville, A.; and Bengio, Y. 2014. Generative Adversarial Nets. In *Proceedings of the 27th International Conference on Neural Information Processing Systems - Volume 2, NIPS14*, 2672–2680.
- Gulrajani, I.; Ahmed, F.; Arjovsky, M.; Dumoulin, V.; and Courville, A. C. 2017. Improved training of wasserstein gans. In *Advances in neural information processing systems*, 5767–5777.
- Isola, P.; Zhu, J.-Y.; Zhou, T.; and Efros, A. A. 2017. Image-to-Image Translation with Conditional Adversarial Networks. *2017 IEEE Conference on Computer Vision and Pattern Recognition (CVPR)* doi:10.1109/cvpr.2017.632. URL <http://dx.doi.org/10.1109/CVPR.2017.632>.
- Jia, X.; Wei, X.; Cao, X.; and Han, X. 2020. Adv-watermark: A Novel Watermark Perturbation for Adversarial Examples. *arXiv preprint arXiv:2008.01919*.
- Kurakin, A.; Goodfellow, I. J.; and Bengio, S. 2016. Adversarial examples in the physical world. *CoRR abs/1607.0*. URL <http://arxiv.org/abs/1607.02533>.
- Kurakin, A.; Goodfellow, I. J.; and Bengio, S. 2017. Adversarial examples in the physical world. *ArXiv abs/1607.02533*.
- Lee, M.; and Kolter, J. Z. 2019. On Physical Adversarial Patches for Object Detection. *ArXiv abs/1906.11897*.
- Li, C.; and Wand, M. 2016. Precomputed real-time texture synthesis with markovian generative adversarial networks. In *European conference on computer vision*, 702–716. Springer.
- Li, J.; Schmidt, F. R.; and Kolter, J. Z. 2019. Adversarial camera stickers: {A} physical camera-based attack on deep learning systems. In Chaudhuri, K.; and Salakhutdinov, R., eds., *Proceedings of the 36th International Conference on Machine Learning, {ICML} 2019, 9-15 June 2019, Long Beach, California, {USA}*, volume 97 of *Proceedings of Machine Learning Research*, 3896–3904. PMLR. URL <http://proceedings.mlr.press/v97/li19j.html>.
- Li, X.; and Li, F. 2017. Adversarial examples detection in deep networks with convolutional filter statistics. In *Proceedings of the IEEE International Conference on Computer Vision*, 5764–5772.
- Liu, A.; Liu, X.; Fan, J.; Ma, Y.; Zhang, A.; Xie, H.; and Tao, D. 2019a. Perceptual-Sensitive GAN for Generating Adversarial Patches. In *AAAI*.
- Liu, H.; Ji, R.; Li, J.; Zhang, B.; Gao, Y.; Wu, Y.; and Huang, F. 2019b. Universal Adversarial Perturbation via Prior Driven Uncertainty Approximation. In *The IEEE International Conference on Computer Vision (ICCV)*.
- Liu, X.; Yang, H.; Liu, Z.; Song, L.; Chen, Y.; and Li, H. 2019c. DPATCH: An Adversarial Patch Attack on Object Detectors. *arXiv: Computer Vision and Pattern Recognition*.
- Lu, J.; Issaranon, T.; and Forsyth, D. 2017. Safetynet: Detecting and rejecting adversarial examples robustly. In *Proceedings of the IEEE International Conference on Computer Vision*, 446–454.
- Madry, A.; Makelov, A.; Schmidt, L.; Tsipras, D.; and Vladu, A. 2018. Towards Deep Learning Models Resistant to Adversarial Attacks. In *International Conference on Learning Representations*. URL <https://openreview.net/forum?id=rJzIBfZAb>.
- Meng, D.; and Chen, H. 2017. Magnet: a two-pronged defense against adversarial examples. In *Proceedings of the 2017 ACM SIGSAC conference on computer and communications security*, 135–147.
- Metzen, J. H.; Genewein, T.; Fischer, V.; and Bischoff, B. 2017. On detecting adversarial perturbations. *arXiv preprint arXiv:1702.04267*.

- Montabone, S.; and Soto, A. 2010. Human detection using a mobile platform and novel features derived from a visual saliency mechanism. *Image Vis. Comput.* .
- Moosavi-Dezfooli, S.-M.; Fawzi, A.; and Frossard, P. 2016. DeepFool: A Simple and Accurate Method to Fool Deep Neural Networks. *2016 IEEE Conference on Computer Vision and Pattern Recognition (CVPR)* 2574–2582.
- Papernot, N.; McDaniel, P.; Jha, S.; Fredrikson, M.; Celik, Z. B.; and Swami, A. 2016. The limitations of deep learning in adversarial settings. In *2016 IEEE European Symposium on Security and Privacy (EuroS&P)*, 372–387. IEEE.
- Qiu, H.; Xiao, C.; Yang, L.; Yan, X.; Lee, H.; and Li, B. 2019. Semanticadv: Generating adversarial examples via attribute-conditional image editing. *arXiv preprint arXiv:1906.07927* .
- Salman, H.; Ilyas, A.; Engstrom, L.; Kapoor, A.; and Madry, A. 2020. Do Adversarially Robust ImageNet Models Transfer Better? In *ArXiv preprint arXiv:2007.08489*.
- Sandler, M.; Howard, A.; Zhu, M.; Zhmoginov, A.; and Chen, L.-C. 2018. MobileNetV2: Inverted Residuals and Linear Bottlenecks. *2018 IEEE/CVF Conference on Computer Vision and Pattern Recognition* doi:10.1109/cvpr.2018.00474. URL <http://dx.doi.org/10.1109/CVPR.2018.00474>.
- Shaham, T. R.; Dekel, T.; and Michaeli, T. 2019. SinGAN: Learning a Generative Model From a Single Natural Image. *2019 IEEE/CVF International Conference on Computer Vision (ICCV)* doi:10.1109/iccv.2019.00467. URL <http://dx.doi.org/10.1109/ICCV.2019.00467>.
- Sharif, M.; Bhagavatula, S.; Bauer, L.; and Reiter, M. K. 2016. Accessorize to a Crime: Real and Stealthy Attacks on State-of-the-Art Face Recognition. In *Proceedings of the 2016 ACM SIGSAC Conference on Computer and Communications Security*. Association for Computing Machinery.
- Shocher, A.; Bagon, S.; Isola, P.; and Irani, M. 2019. InGAN: Capturing and Retargeting the “DNA” of a Natural Image. In *Proceedings of the IEEE/CVF International Conference on Computer Vision (ICCV)*.
- Song, Y.; Shu, R.; Kushman, N.; and Ermon, S. 2018. Constructing Unrestricted Adversarial Examples with Generative Models. In Bengio, S.; Wallach, H.; Larochelle, H.; Grauman, K.; Cesa-Bianchi, N.; and Garnett, R., eds., *Advances in Neural Information Processing Systems 31*, 8312–8323. Curran Associates, Inc. URL <http://papers.nips.cc/paper/8052-constructing-unrestricted-adversarial-examples-with-generative-models.pdf>.
- Su, J.; Vargas, D. V.; and Sakurai, K. 2019. One pixel attack for fooling deep neural networks. *IEEE Transactions on Evolutionary Computation* .
- Szegedy, C.; Liu, W.; Jia, Y.; Sermanet, P.; Reed, S.; Anguelov, D.; Erhan, D.; Vanhoucke, V.; and Rabinovich, A. 2015a. Going deeper with convolutions. *2015 IEEE Conference on Computer Vision and Pattern Recognition (CVPR)* doi:10.1109/cvpr.2015.7298594. URL <http://dx.doi.org/10.1109/CVPR.2015.7298594>.
- Szegedy, C.; Vanhoucke, V.; Ioffe, S.; Shlens, J.; and Wojna, Z. 2015b. Rethinking the Inception Architecture for Computer Vision. *CoRR* abs/1512.00567. URL <http://arxiv.org/abs/1512.00567>.
- Szegedy, C.; Zaremba, W.; Sutskever, I.; Bruna, J.; Erhan, D.; Goodfellow, I. J.; and Fergus, R. 2014. Intriguing properties of neural networks. *CoRR* abs/1312.6199.
- Tan, M.; Chen, B.; Pang, R.; Vasudevan, V.; Sandler, M.; Howard, A.; and Le, Q. V. 2019. MnasNet: Platform-Aware Neural Architecture Search for Mobile. *2019 IEEE/CVF Conference on Computer Vision and Pattern Recognition (CVPR)* doi:10.1109/cvpr.2019.00293. URL <http://dx.doi.org/10.1109/CVPR.2019.00293>.
- Thys, S.; Ranst, W. V.; and Goedeme, T. 2019. Fooling Automated Surveillance Cameras: Adversarial Patches to Attack Person Detection. *2019 IEEE/CVF Conference on Computer Vision and Pattern Recognition Workshops (CVPRW)* doi:10.1109/cvprw.2019.00012. URL <http://dx.doi.org/10.1109/CVPRW.2019.00012>.
- Tramèr, F.; Kurakin, A.; Papernot, N.; Boneh, D.; and McDaniel, P. D. 2018. Ensemble Adversarial Training: Attacks and Defenses. *ArXiv* abs/1705.07204.
- Wiyatno, R. R.; and Xu, A. 2019. Physical Adversarial Textures That Fool Visual Object Tracking. In *The IEEE International Conference on Computer Vision (ICCV)*.
- Xu, W.; Evans, D.; and Qi, Y. 2017. Feature squeezing: Detecting adversarial examples in deep neural networks. *arXiv preprint arXiv:1704.01155* .
- Zhu, J.-Y.; Park, T.; Isola, P.; and Efros, A. A. 2017. Unpaired image-to-image translation using cycle-consistent adversarial networks. In *Proceedings of the IEEE international conference on computer vision*, 2223–2232.